Molecular & Biochemical Parasitology 191 (2013) 66–74

Contents lists available at ScienceDirect

Molecular & Biochemical Parasitology

Insights into the regulation of GPEET procyclin during differentiation from early to late procyclic forms of *Trypanosoma brucei*

Sebastian Knüsel[a,b], Isabel Roditi[a,*]

[a] Institute of Cell Biology, University of Bern, Baltzerstrasse 4, CH-3012 Bern, Switzerland
[b] Graduate School of Cellular and Biomedical Sciences, University of Bern, Freiestrasse 1, CH-3012 Bern, Switzerland

ARTICLE INFO

Article history:
Received 8 August 2013
Received in revised form
17 September 2013
Accepted 18 September 2013
Available online 27 September 2013

Keywords:
Trypanosoma brucei
Procyclin
Differentiation
RNA stability
3′ UTR
Uridylation

ABSTRACT

The procyclic form of *Trypanosoma brucei* colonises the gut of its insect vector, the tsetse fly. GPEET and EP procyclins constitute the parasite's surface coat at this stage of the life cycle, and the presence or absence of GPEET distinguishes between early and late procyclic forms, respectively. Differentiation from early to late procyclic forms *in vivo* occurs in the fly midgut and can be mimicked in culture. Our analysis of this transition *in vitro* delivered new insights into the process of GPEET repression. First, we could show that parasites followed a concrete sequence of events upon triggering differentiation: after undergoing an initial growth arrest, cells lost GPEET protein, and finally late procyclic forms resumed proliferation. Second, we determined the stability of both *GPEET* and *EP* mRNA during differentiation. *GPEET* mRNA is exceptionally stable in early procyclic forms, with a half-life >6 h. The *GPEET* mRNA detected in late procyclic form cultures is a mixture of transcripts from both *bona fide* late procyclic forms and GPEET-positive 'laggard' parasites present in these cultures. However, its stability was clearly reduced during differentiation and in late procyclic form cultures. Alternatively processed *GPEET* transcripts were enriched in samples from late procyclic forms, suggesting that altered mRNA processing might contribute to repression of GPEET in this developmental stage. In addition, we detected *GPEET* transcripts with non-templated oligo(U) tails that were enriched in late procyclic forms. To the best of our knowledge, this is the first study reporting a uridylyl-tailed, nuclear-encoded mRNA species in trypanosomatids or any other protozoa.

1. Introduction

The kinetoplastid parasite *Trypanosoma brucei*, the causative agent of African sleeping sickness in humans and Nagana in livestock, relies on the tsetse fly for transmission. Since *T. brucei* colonises both hosts and different tissues within a host, it requires robust mechanisms that allow it to adapt its gene expression to alterations in the environment. To enable infection of tsetse, the proliferating long slender bloodstream forms first need to differentiate to cell-cycle arrested short stumpy forms [1]. These express a specific set of genes pre-adapting them for transfer to the tsetse fly, notably genes associated with mitochondrial metabolism [2–6]. When the fly ingests a blood meal, stumpy forms differentiate to procyclic forms (PF) in the lumen of the midgut [7]. In culture, this differentiation can be mimicked by a drop in temperature of ≥10 °C and exposure to citrate/*cis*-aconitate [8]. As they differentiate, the parasites shed their coat of variant surface glycoproteins (VSG) [9,10] and replace it by two classes of procyclins that are distinguished by their internal dipeptide (EP) and pentapeptide (GPEET) repeats [11–14]. Trypanosomes subsequently meet one of two fates: the parasites are either eliminated after a few days, or they migrate to and colonise the ectoperitrophic space surrounding the midgut (reviewed in [15]).

During tsetse fly infection, parasites only transiently express GPEET procyclin, and the presence or absence of GPEET distinguishes between early and late PF, respectively. GPEET is repressed between 4 and 7 days after ingestion, while EP continues to be expressed [16]. GPEET repression coincides with the parasite's migration to the ectoperitrophic space, but it is not known whether down-regulation of GPEET is required for this step. The same sequence of events is observed when bloodstream forms are triggered to differentiate to PF in culture, with GPEET and all isoforms of EP (EP1, EP2, EP3) being expressed within a few hours after differentiation is triggered [17,18]. While expression of GPEET can be prolonged in medium containing glycerol, repression occurs after about 11 days in medium without glycerol; this transition from GPEET-positive to GPEET-negative cells is accompanied by a transient growth arrest [16].

Abbreviations: ActD, actinomycin D; EdU, 5-ethynyl-2′-deoxyuridine; GRE, glycerol responsive element; PF, procyclic form; SBPW, saponin-based permeabilisation and wash reagent; $t_{1/2}$, half-life; U, uridine; UTR, untranslated region; VSG, variant surface glycoprotein.

* Corresponding author. Tel.: +41 31 631 4647; fax: +41 31 631 4684.
E-mail address: isabel.roditi@izb.unibe.ch (I. Roditi).

0166-6851/$ – see front matter © 2013 Elsevier B.V. All rights reserved.
http://dx.doi.org/10.1016/j.molbiopara.2013.09.004

Several studies demonstrated that GPEET expression responds to the environment, linking its regulation to nutrient availability and central metabolism: the presence of glycerol and low concentration of glucose promote GPEET expression, while hypoxia accelerates GPEET repression [16,19]. Furthermore, the activity of mitochondrial enzymes was shown to control expression of GPEET [20]. A *cis*-regulatory element in the 3′ untranslated region (UTR), known as the glycerol responsive element (GRE), destabilises *GPEET* mRNA in the fly gut and in culture in response to high glucose concentration or glycerol deprivation [20,21]. Other environmental factors may also act via the GRE and hence lead to reactivation of GPEET in culture; for example, different serum components might explain the variation in GPEET expression observed between and within different strains of *T. brucei* [22].

Analysis of GPEET expression in tsetse and in culture revealed that in late PF *GPEET* mRNA is undetectable, or only present at very low levels [16,21,23]. The repression of GPEET occurs post-transcriptionally, as the promoter remains active in late PF [16]. Procyclins are transcribed by RNA polymerase I in the nucleolus, and it was recently shown that proteins involved in ribosomal RNA maturation also regulate GPEET expression [23]. Thus, at least part of the regulation may take place before the mature mRNA is exported and reaches the cytoplasm.

The stability of bulk procyclin mRNA was previously measured in bloodstream forms and PF [24,25], and turnover of *EP1* mRNA in bloodstream forms was determined by means of reporter mRNAs [26–30]. However, these studies either did not discriminate between *GPEET* and *EP*, or lacked data on *GPEET* mRNA in general; in addition, procyclin mRNA stability has never been assessed during the transition from early to late PF.

The present study reveals that, despite being very similar in sequence, *GPEET* and *EP* mRNA stability is regulated independently during differentiation and that *GPEET* mRNA can be detected and measured in late PF. We also elucidated the timing of events during differentiation to late PF: initially, GPEET-positive parasites stop dividing, followed by repression of GPEET, and GPEET-negative cells eventually resume proliferation. Furthermore, mapping mRNA 3′ ends identified alternatively processed *GPEET* transcripts; besides poly(A)-tailed and deadenylated mRNAs, we detected extended 3′ UTRs lacking tails, different 3′ ends within the 3′ UTR and non-templated oligo(U)-tailed transcripts.

2. Materials and methods

2.1. Cell culture

This study was performed using the pleomorphic, fly-transmissible strain *Trypanosoma brucei brucei* AnTat1.1 [31]. Bloodstream forms were obtained from mouse blood after transmission through tsetse as described [32]. Differentiation to early PF was triggered in DTM [33] supplemented with 15% FBS and 6 mM *cis*-aconitate at 27 °C [34]. The culture was expanded in DTM + 15% FBS and stabilates were stored in liquid nitrogen 8–12 days after triggering differentiation. Before differentiation to late PF, stabilates of early PF were thawed and cultured for 3 days in DTM + 15% FBS with daily dilution to 3×10^6 cells ml^{-1}. The culture was diluted ~4× in SDM-79 [35] supplemented with 10% FBS and 20 mM glycerol to a concentration of 3×10^6 cells ml^{-1} and expanded for 4 days in SDM-79 + 10% FBS and 20 mM glycerol with daily dilution to 3×10^6 cells ml^{-1}.

Differentiation to late PF was triggered by washing trypanosomes twice in SDM-79 + 10% FBS lacking glycerol [16]. Cells were diluted to 4×10^6 cells ml^{-1} on the day of glycerol removal and cultured in SDM-79 + 10% FBS with daily dilution to 7×10^6 cells ml^{-1} on subsequent days. Cultures were grown in 150 cm^2 tissue culture flasks with vent screw cap (TPP, Switzerland) in a total volume of 75 ml.

2.2. RNA isolation and Northern blotting

To determine mRNA stability, cultures with a density of 7×10^6 cells ml^{-1} were incubated with 10 μg ml^{-1} Actinomycin D (ActD) for the indicated time, including 10 min of centrifugation. Total RNA was extracted from 1.5×10^8 cells with guanidine thiocyanate [36]. Northern blot analysis of 10 μg total RNA per lane was performed as described [11]. *GPEET* (Tb927.6.510) and *EP* mRNA were detected using Mega-Prime-^{32}P-labelled hybridisation probes (Amersham Biosciences, UK). The genome encodes several copies of *EP* on chromosomes 6 and 10.

Primer sequences used to create the labelling template by PCR amplification: MicroarrPROs (5′-GCTATGACCATGGCGTGGGATTTGCC) and MicroarrPROas (5′-GATTTCAGCGTTGCAGCACCAG) for both *GPEET* and *EP1*, flanking an internal region encoding the pentapeptide and dipeptide repeats, respectively [20]. Hybridisation was performed at 60 °C in solution containing 50% formamide and blots were washed at 55 °C in solution containing 0.2× SSC and 0.1% SDS. ^{32}P-labelled oligonucleotides were used to detect 18S rRNA as a control for sample loading [37]. Radioactive blots were exposed to X-ray film and Phosphorimager screen (Amersham Biosciences, UK; scanned with a Storm 820) for quantitation (AIDA 3.11 software by Raytest, Germany).

2.3. Flow cytometry analysis

Expression of GPEET was monitored by flow cytometry as described [11,33]. The following procedure was performed at 4 °C: cells were washed once in PBS and blocked in 2% BSA in PBS for 1 h. 2×10^6 cells were incubated with polyclonal rabbit antiserum K1 (1:1000) [38] and Alexa Fluor 488-conjugated goat anti-rabbit IgG (1:1000; Invitrogen) secondary antibody in 2% BSA/PBS for 30 min each. After each antibody incubation, cells were pelleted at 3300 g for 2 min and washed three times in cold PBS. Fluorescence of 10 000 cells was measured with a FACSCalibur™ and quantified using CellQuest Pro 5.2 (both BD Biosciences).

2.4. Proliferation assay and fluorescence microscopy

Proliferating cells were labelled using the Click-iT® EdU Flow Cytometry Assay Kit (Invitrogen). 5-ethynyl-2′-deoxyuridine (EdU) was dissolved in DMSO to obtain a 0.3 M 1000× stock solution. The experiment was performed according to manufacturer's protocol, with minor adaptations. 7×10^6 cells were incubated with 0.3 mM EdU in 1 ml culture medium in a humid chamber at 27 °C. Cells were harvested after 24 h and pelleted at 3300 g for 2 min. The following procedure was performed at room temperature: after sequential washing in 1% BSA/PBS and PBS only, cells were resuspended in 250 μl PBS and fixed for 15 min by addition of 250 μl 8% paraformaldehyde in PBS. After sequential washing in PBS, 1% BSA/PBS and 1× saponin-based permeabilisation and wash reagent (1× SBPW, supplied with kit), cells were resuspended in 40 μl 1× SBPW and permeabilized for 5 min. Incorporated EdU was fluorescently labelled by addition of 200 μl Click-iT cocktail (supplied with kit; containing Alexa Fluor 488 azide) and incubation for 30 min. After sequential washing in 1× SBPW and PBS only, GPEET expression was monitored as described in Section 2.3, using Cy™ 3-conjugated goat anti-rabbit IgG (1:1000; Jackson Immuno Research, Pennsylvania, USA) as secondary antibody. Fluorescence was quantified as described in Section 2.3. For microscopy, 10^6 cells were allowed to settle for 20 min on coverslips and mounted in Moviol 4-88 (Hoechst) containing 1.5 μg ml^{-1} DAPI. Images were

acquired with a DFC350 FX monochrome CCD camera mounted on a DM6000B microscope (Leica). Images were superimposed and analysed using LAS AF software (Leica).

2.5. mRNA 3′ end mapping

3′ ends of *GPEET* mRNA were mapped using the ALL-TAIL™ Kit For Extreme 3′ RACE (Bioo Scientific, TX, USA) according to manufacturer's protocol: 1 μg of DNAse I-treated total RNA was ligated to an adenylated linker oligonucleotide (Linker C) in 20 μl reaction volume for 1 h at 22 °C. 4 μl of ligation reaction was used for reverse transcription in 20 μl reaction volume for 30 min at 42 °C, using a primer complementary to the linker oligonucleotide (Linker C Rev). After heat-inactivation for 5 min at 92 °C, 1 μl of cDNA was used as template in a *GPEET*-specific PCR in a final volume of 25 μl (annealing temperature: 50 °C; extension time: 2.5 min; 35 cycles; primers used: GPEET P1 F 5′-TCGGCTAGCAACGTTATCGTG and Linker C Rev 5′-CTGGAATTCGCGGTTAAA). As *GPEET* mRNA abundance is very low in late PF, a hemi-nested PCR was performed (Primers Proc P3 F 5′-TGGTGCTGCAACGC and Linker C Rev), using a 1:300 dilution of the *GPEET*-specific PCR as template (identical PCR conditions). PCR products were cloned in pGEM T-Easy (Promega) and individual colonies sequenced by Sanger sequencing (Microsynth, Switzerland).

3. Results

3.1. Cells that resume proliferation during differentiation are GPEET-negative

Early PF express GPEET procyclin on their surface and can be triggered to differentiate to GPEET-negative late PF by removal of glycerol from the culture medium. Both early and late PF of AnTat1.1 have a population doubling time of ~17 h in culture. One to two days after early PF were triggered to differentiate, the population underwent a growth arrest for 4–6 days (Fig. 1A and [16]). As determined in this previous study, 86% of early PF entered S phase of the cell cycle and incorporated BrdU into the DNA. In contrast, only 18% of the cells were BrdU-positive 6 days after initiation of differentiation, which is consistent with the observed growth inhibition. Furthermore it was shown that repression of GPEET was asynchronous, with single cells switching off GPEET individually [16].

We therefore tested the hypothesis that early PF stopped dividing before down-regulating GPEET and resumed proliferation once they become GPEET-negative. A two-colour flow cytometry protocol was established to simultaneously detect early PF labelled with a GPEET-specific antibody and proliferating cells by incorporation of the thymidine analogue EdU, which can be covalently linked to a fluorophore. Early PF were triggered to differentiate and analysed by flow cytometry. Samples were taken from both early (d 0) and late (d 13) PF, as well as at two time points corresponding to an early and a late phase of growth arrest (d 3 and d 6, respectively; Fig. 1A). The specificity of the detection method was confirmed by assaying early PF for incorporation of EdU or GPEET expression alone (data not shown) and by incubating cells without anti-GPEET anti-serum or EdU (Fig. 1B).

The kinetics of GPEET repression during differentiation was as expected: in a culture of early PF (d 0), 92.5% of cells were GPEET-positive (Fig. 1C). Following initiation of differentiation, 83.6% of cells expressed GPEET on d 3 and 52.7% on d 6, whereas only 3.3% were GPEET-positive in a culture of late PF (d 13). With regard to proliferation, 74.2% of cells incorporated EdU on d 0, with 73.1% being positive for GPEET (Fig. 1C). Shortly after the reduction in growth became obvious (d 3), only 18.3% of the population entered

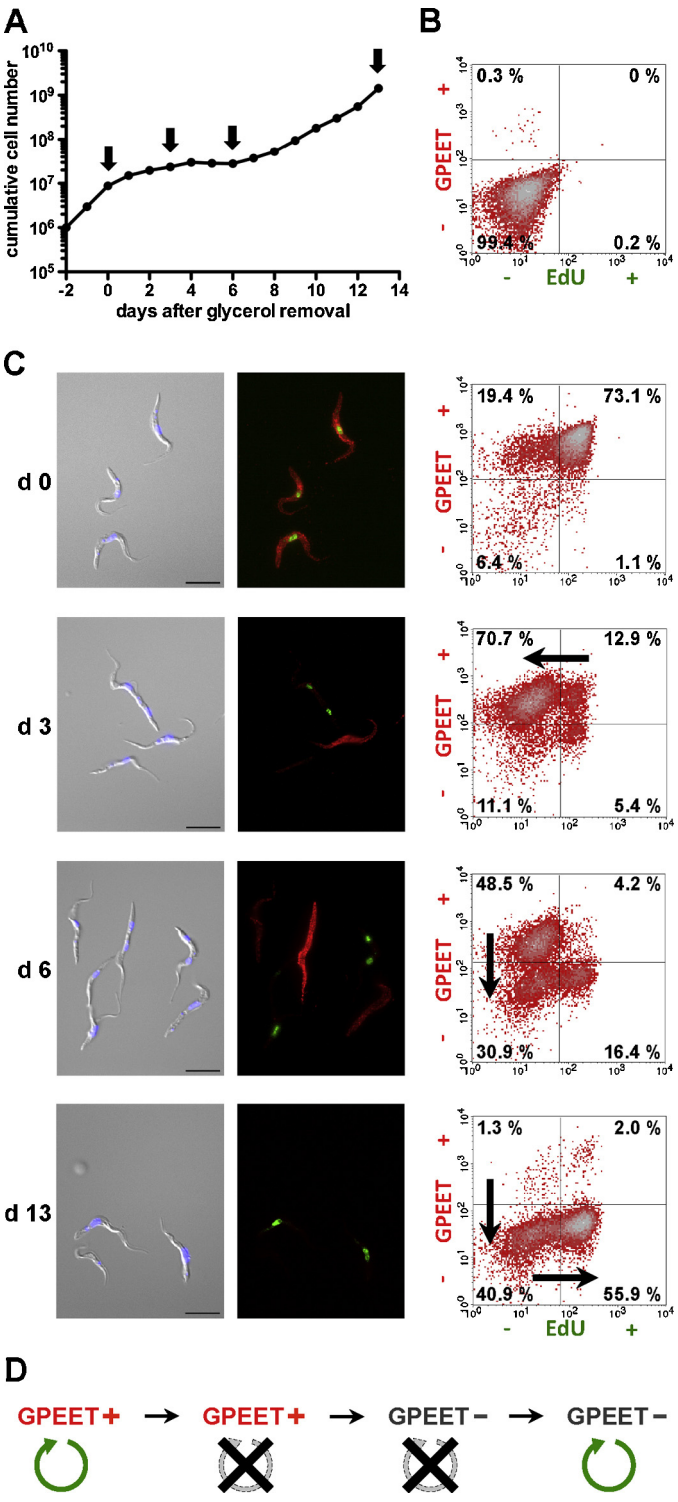

Fig. 1. Proliferation and GPEET expression during differentiation. (A) Growth during *in vitro* differentiation from early to late PF. Differentiation was triggered on d 0. Arrows indicate time points where samples were taken for flow cytometry analysis of proliferation and GPEET protein expression. (B and C) Two-colour flow cytometric analysis of samples described above; *x*-axis: EdU labels proliferating cells, *y*-axis: GPEET protein expression. (B) Early PF (d 0), incubated without anti-GPEET anti-serum or EdU. (C) Quantification of all samples taken during differentiation. Arrows indicate the main population's shift to a different quadrant in respect to the previous sample. Merges of corresponding microscope images are shown; left: DIC and DNA (DAPI, blue), right: anti-GPEET (red) and EdU-Alexa488 (green). Scale bar: 10 μm. (D) Sketch summarising the sequence of events observed by flow cytometry analysis. Circular arrows depict proliferation.

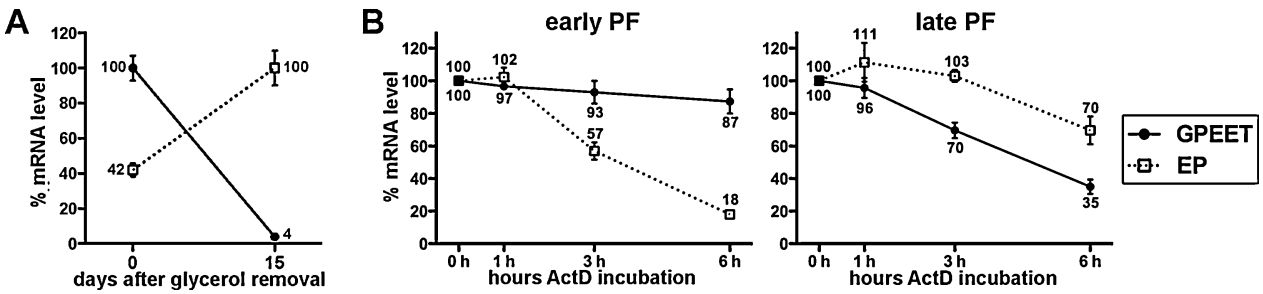

Fig. 2. Half-life of procyclin mRNA in early and late procyclic forms. (A and B) Relative mRNA levels of *GPEET* (filled circles, solid line) and *EP* (empty squares, dotted line), determined by Northern blotting. Samples were normalised against 18S rRNA. Means and standard deviations are displayed, $n = 3$. (A) Steady-state mRNA levels in early (d 0) and late (d 15) PF. (B) mRNA levels after incubation with ActD for the indicated times in early PF (left) and late PF (right), relative to steady state levels (0 h ActD).

S phase during an incubation period of 24 h. Of the cells that incorporated EdU, approximately two-thirds still expressed GPEET (12.9%), while one-third had already repressed it (5.4%). Moreover, the cells that stopped dividing were mainly GPEET-positive (70.7%), indicating that growth arrest preceded down-regulation of GPEET. After 6 days of differentiation, an increase in GPEET-negative quiescent cells was observed: from 11.1% on d 3 to 30.9% on d 6. Although the total fraction of parasites incorporating EdU remained similar (18.3% on d 3 and 20.6% on d 6), the distribution shifted towards incorporation of EdU by cells that had lost GPEET (16.4% GPEET-negative compared to 4.2% GPEET-positive cells). Resumption of proliferation was observed after cells had completed differentiation: while 57.9% of cells incorporated EdU on d 13, only 2% were also GPEET-positive. In summary: it appeared that the sequence of events started with an arrest in proliferation of GPEET-positive cells, followed by down-regulation of GPEET in quiescent cells and continuation of proliferation by GPEET-negative parasites (Fig. 1D). This scenario implies that 'laggard' parasites, which repress GPEET at a later time than the majority of the population, might well be part of the community of late PF, but eventually they will be outgrown by the progeny of differentiated parasites.

3.2. The steady-state level and half-life of GPEET mRNA are reduced during differentiation and in late procyclic forms

Distinct elements regulating mRNA stability and translation have been mapped within the procyclin 3′ UTR [24,25,30,39]. The 3′ UTR of *GPEET* harbours the GRE, a negative element conferring mRNA instability, thus leading to a transcript that is barely detected or even absent in late PF [16,20,23]. We decided to recapitulate these results and assess the relative steady-state levels and the stability of *GPEET* mRNA in both early and late PF. Triplicate cultures of early PF (d 0) were incubated with 10 μg ml^{-1} ActD to block transcription, and RNA was extracted after 0, 1, 3 and 6 h. Untreated aliquots were triggered to differentiate and RNA was extracted from late PF (d 15) after 0, 1, 3 and 6 h of incubation with ActD. Analysis of both stages by flow cytometry yielded the expected proportion of GPEET-positive cells: 90–91% in early PF and 2–4% in late PF (data not shown).

Northern blotting was performed to determine the mRNA levels of *GPEET* and *EP*; Fig. 2A and B show quantifications of the corresponding experiments. *GPEET* mRNA abundance in late PF was reduced more than 25-fold compared to early PF (Fig. 2A). In contrast, steady-state levels of *EP* mRNA were increased by 2.4-fold in late PF. *GPEET* mRNA displayed a half-life ($t_{1/2}$) of more than 6 h in early PF and was still surprisingly stable in late PF with a $t_{1/2}$ of 3.80 h ± 0.32 (Fig. 2B). The opposite was observed for *EP* mRNA: while the $t_{1/2}$ was determined to be 2.31 h ± 0.11 in early PF, it was greater than 6 h in late PF (Fig. 2B).

We next investigated the abundance and stability of procyclin mRNAs during the course of differentiation from early to late PF. Cells were triggered to differentiate and assessed for GPEET protein expression in cultures from early PF (d 0) and 2, 4, 6, 8 and 11 days after glycerol removal. On the same days cultures were incubated for 0, 1, 3 and 6 h with ActD and RNA was extracted to determine mRNA stability. Data from three independent experiments were analysed; results from one experiment are shown in Figs. 3 and 4.

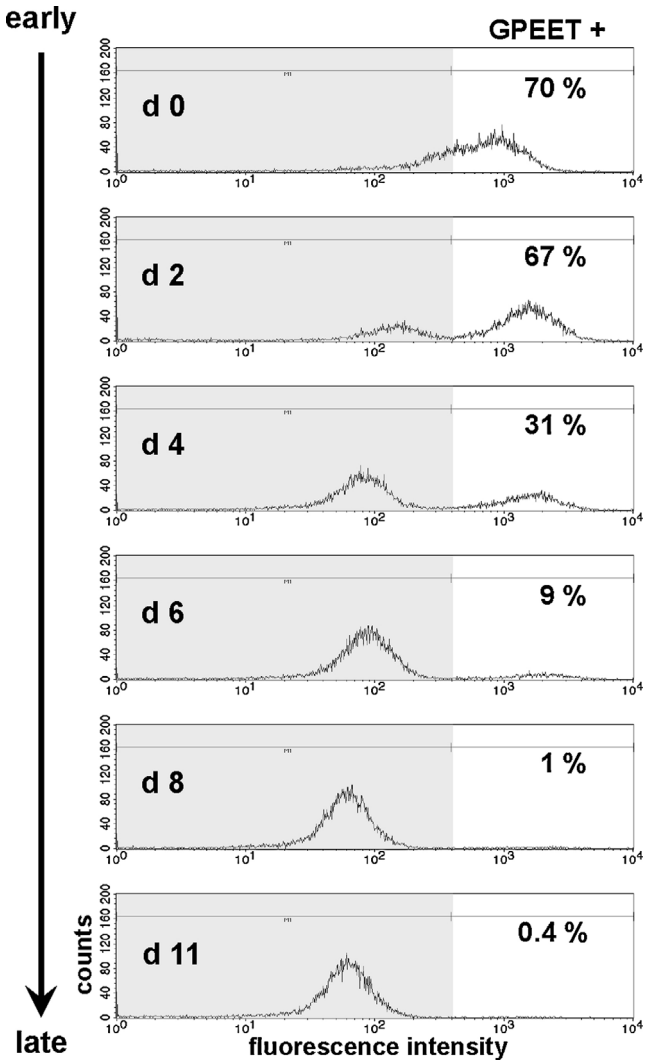

Fig. 3. GPEET protein expression during differentiation. Flow cytometric analysis of GPEET protein expression during differentiation from early PF (d 0, top) to late PF (d 11, bottom). Numbers in percent: proportion of GPEET-positive cells. Three independent experiments were performed: graphs from one experiment are shown; see Supplemental Figs. S1 and S2 for data from the other two experiments.

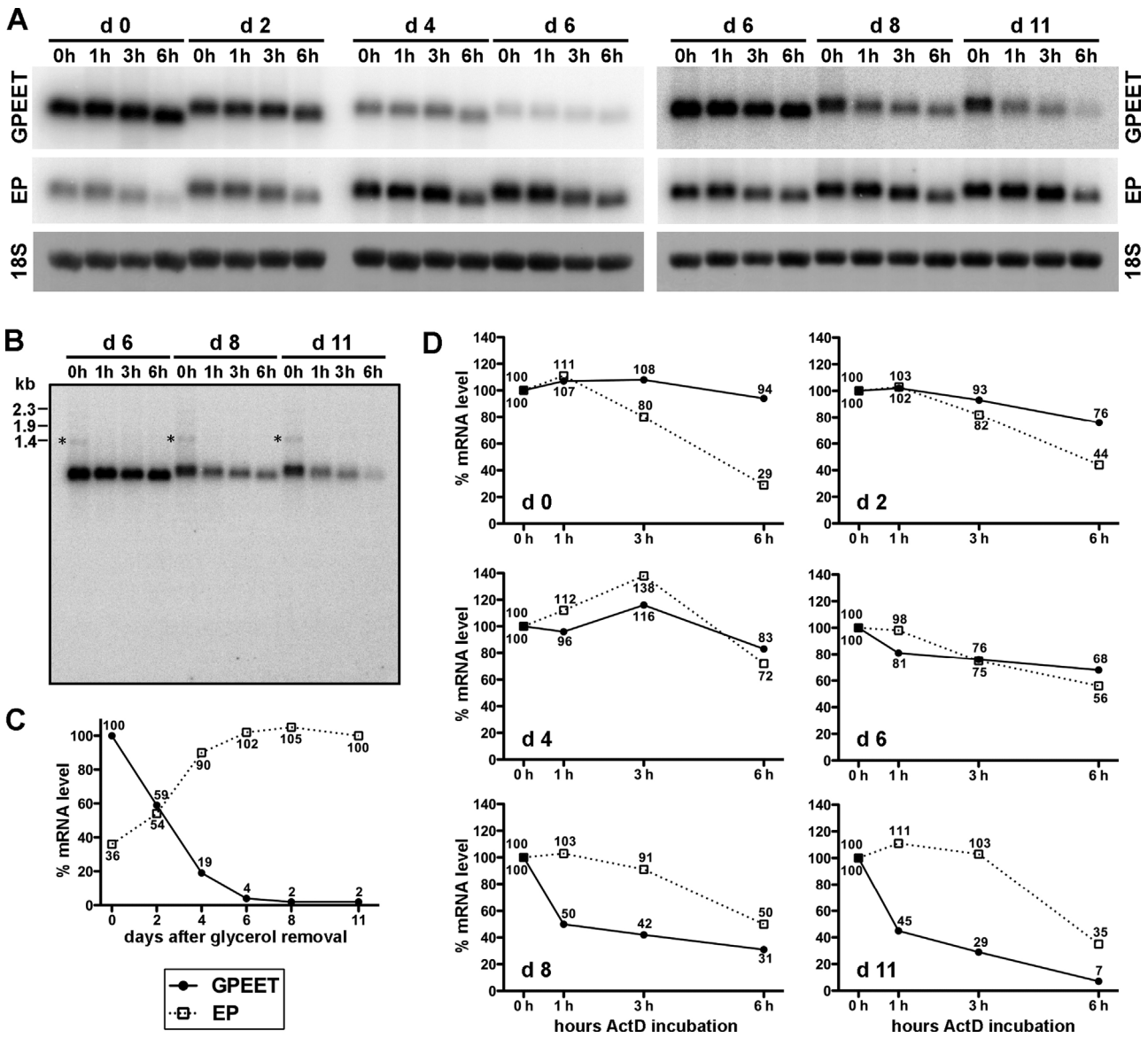

Fig. 4. Stability of procyclin mRNA during differentiation. (A) Northern blot analysis of *GPEET* and *EP* during differentiation form early PF (d 0) to late PF (d 11); samples were derived from the same cultures that were analysed by flow cytometry in Fig. 3. RNA was extracted after incubation with ActD for the times indicated. To accommodate all samples, two gels were used. Samples from d 6 were loaded on both gels to obtain reference levels. Blots were exposed for different lengths of time. 18S rRNA was used for normalisation. (B) Northern blot analysis of *GPEET* on day 6, 8 and 11, as described above. A larger section of the blot illustrated in (A) is shown. Asterisks mark additional bands of ~1.4 kb. The sizes of rRNAs are marked. (C and D) Quantification of Northern blots from (A). Relative mRNA levels of *GPEET* (filled circles, solid line) and *EP* (empty squares, dotted line) are shown. (C) Steady-state mRNA levels during differentiation from early (d 0) to late PF (d 11). (D) mRNA levels after incubation with ActD for the indicated times, relative to steady state levels (0 h ActD). Three independent experiments were performed: graphs from one experiment are shown; see Supplemental Figs. S1 and S2 for data from the other two experiments.

Data from the other two sets of experiments are provided in Supplemental Figs. S1 and S2.

Supplementary material related to this article can be found, in the online version, at http://dx.doi.org/10.1016/j.molbiopara.2013.09.004.

Flow cytometry analysis demonstrated the down-regulation of GPEET protein from 70% GPEET-positive cells in early PF (d 0) to 0.4% in late PF (d 11) (Fig. 3). As described before [16], no intermediate levels of GPEET expression were observed, indicating a rapid transition and loss of GPEET by individual cells. To quantify the stability and relative abundance of procyclin mRNAs from all samples, Northern blotting was performed on two separate gels. RNA samples from d 6 were loaded on both gels to provide reference levels; the two blots were exposed for different lengths of time to enable detection of the whole spectrum of *GPEET* mRNA during differentiation (Fig. 4A). Probing for both *EP* and *GPEET* mRNAs resulted in detection of a single band of ~800 bases in size. This band appeared to shorten from 0 h to 6 h of ActD incubation on all days analysed, but it was less prominent on d 6. A *GPEET* transcript of ~1.4 kb was observed in untreated samples, particularly from cultures in the later phases of differentiation (0 h ActD of d 6, d 8 and d 11), but no stable degradation intermediates could be detected (Fig. 4B).

In this experiment, steady-state levels of *GPEET* mRNA decreased more than 50-fold from early to late PF, while *EP* increased by 2.8-fold (Fig. 4C). As seen in the previous experiment (Fig. 2B), *GPEET* mRNA was extremely stable in early PF (d 0) and became progressively less stable during differentiation (Fig. 4D). In late PF (d 11), seven percent of the mRNA was detectable after 6 h of incubation with ActD. In contrast to the previous experiment,

biphasic kinetics of degradation were observed on d 8 and d 11: within 1 h of inhibition of transcription, there was a steep drop in mRNA level below 50%; the remaining mRNA appeared to be degraded more slowly. In addition, the stability of *EP* mRNA in this experiment was comparable in both early and late PF and appeared to be slightly more stable during differentiation (d 2–8). The discrepancies between different experiments might be explained by the different proportion of GPEET-positive parasites present in the cultures of late PF. Nevertheless, we were able to show that *GPEET* mRNA can still be detected in late PF cultures harbouring <1% GPEET-positive cells and that its stability is greatly reduced during differentiation to late PF.

In some samples we measured an increase in mRNA abundance up to 3 h after the addition of ActD (Fig. 4D, panel d 4 and Fig. S1, panels d 0, d 2, d 6, d 11). Transient rises up to 2 h have been observed in kinetoplastids [40] and have been attributed to a pool of precursors that continue to be spliced after transcription is inhibited [27]. We propose that the prolonged rise observed with procyclin mRNAs is due to their extraordinary stability.

3.3. Mapping *GPEET* mRNA 3′ ends reveals transcript deadenylation and addition of oligo-uridylyl tails

Northern blotting revealed a shortening of procyclin transcripts after 6 h incubation with ActD (Fig. 4A and B), which would be consistent with deadenylation of mRNAs. To test this, we mapped *GPEET* mRNA 3′ ends from early and late PF at 0 h and 6 h after addition of ActD. After ligation of an anchor oligonucleotide to the 3′ hydroxyl group of total RNA, cDNA was obtained by reverse transcription using a primer complementary to the anchor. *GPEET*-specific products were amplified in two sequential PCRs, cloned and analysed by Sanger sequencing (as this is the only method to give accurate lengths of poly(A) tails). For both early and late PF, 48 clones from untreated samples (0 h ActD) were sequenced, while 96 clones were sequenced from samples obtained 6 h after addition of ActD. It is worth noting that although the number of clones that mapped to individual 3′ ends is given, our method yields semi-quantitative rather than quantitative information.

Overall, most of the clones contained (poly)adenylated 3′ ends, but fewer clones with poly(A) tails were obtained from samples of late PF (Fig. 5A). A clear shift towards a shorter poly(A) tail, or no tail, was observed in samples after 6 h incubation with ActD. We also identified three alternative poly(A) sites, located in close proximity to the major polyadenylation site [41] (Fig. 5B). These minor poly(A) sites were also reported in previous studies using RNA-Seq technology [42,43].

The method employed to map 3′ ends of mRNAs would also identify non-adenylated transcripts and degradation intermediates bearing a 3′ hydroxyl group. Indeed, we obtained 9 clones from untreated samples of late PF that harboured non-adenylated 3′ ends extending beyond the major polyadenylation site, the longest one being 554 nucleotides (Fig. 5B). Four out of 9 extended 3′ UTRs ended within or downstream of the putative novel transcript *Tb6.NT.31* [43], but did not coincide with its annotated polyadenylation sites. The discrete band of ~1.4 kb, observed by Northern blotting of untreated samples on d 6, d 8 and d 11 (Fig. 4B), was not detected in these experiments, however.

The 3′ ends of 52 non-adenylated sequences mapped to 9 different sites within the 3′ UTR (Fig. 6A and B). Five of these (sites 1, 2, 7, 8, 9) were found uniquely in the sample from untreated late PF and one (site 5) was only identified in early PF when parasites were treated with ActD for 6 h. Three sites (sites 3, 4, 6) were found in more than one of the samples analysed. Two of these (sites 3 and 4) were located within the GRE, with one site (site 4) being clearly enriched in samples from late PF after 6 h of incubation with ActD (Fig. 6A and B). Sites 3 and 6 must be treated with caution, however, as they might result from priming artifacts during reverse transcription. Pilot experiments with different anchors showed that, instead of pairing with the ligated anchor oligonucleotide, the primer can anneal to internal sequences of an RNA molecule if the 3′ end of the primer has perfect complementarity to four nucleotides.

Most interestingly, we obtained clones that harboured non-templated oligo-uridylyl tails at three different locations (sites A, B, and C) near the end of the 3′ UTR (Fig. 6A and C). The single clone that had a tail at site B was obtained from late PF after 6 h of ActD incubation. The three non-templated uridines (Us) were preceded by an encoded stretch of 8 Us. Tails at site A were only found in untreated samples from early PF cultures and harboured between 9 and 13 non-templated Us, preceded by a stretch of 4 encoded Us. Finally, we obtained clones from three out of four samples that had a tail length of 8–12 non-templated Us at site C, located two nucleotides upstream of the major polyadenylation site. These tails were primarily found in samples after 6 h of incubation with ActD in both early and late PF, but were clearly enriched in late PF (Fig. 6A and C). The early and late PF cultures used for RNA preparation were never exclusively GPEET-positive or GPEET-negative, respectively. Thus mixed populations of early and late PF could explain why some 3′ ends were not restricted to samples from late PF cultures, although they might be specific to cells that have repressed GPEET.

It has been drawn to our attention that the Linker C Rev primer used for RT-PCR in this analysis ended with 3 adenosine residues

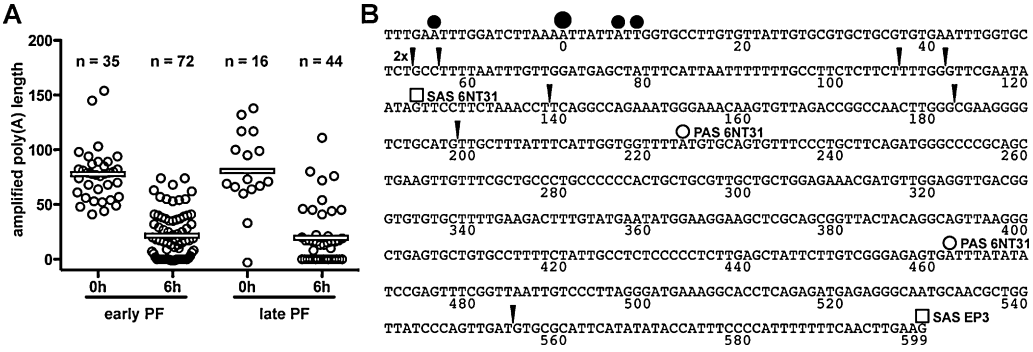

Fig. 5. Mapping *GPEET* mRNA 3′ ends reveals transcript deadenylation and extended 3′ UTRs. (A) Lengths of poly(A) tails in early and late PF after incubation with ActD for 0 h and 6 h. Numbers of clones containing (poly)adenylated 3′ ends are indicated, white bars represent mean values. Number of clones sequenced: 48 for samples after 0 h ActD, 96 for samples after 6 h ActD. (B) Location of polyadenylation sites (filled circles, obtained from all samples analysed) and non-adenylated extended 3′ UTRs (filled arrowheads, only found in untreated late PF). Sequence encompassing the *GPEET-EP3* intergenic region obtained from *T. brucei* strain Tb927 (tritrypdb.org) is shown, relative to the major polyadenylation site (position 0, big filled circle). Annotated landmarks of the putative novel transcript *Tb6.NT.31* [43] and *EP3* are shown for orientation: splice acceptor sites (SAS, empty squares) and polyadenylation sites (PAS, empty circles), obtained from [43].

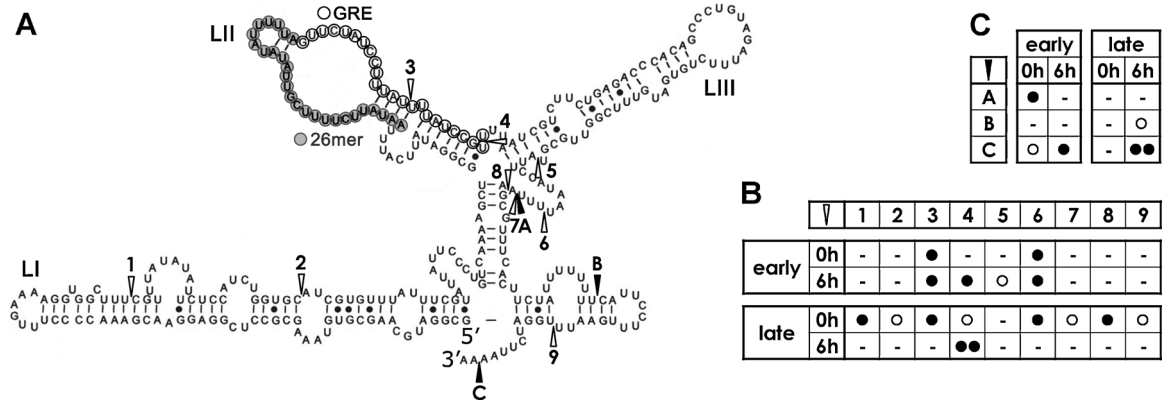

Fig. 6. Location of 3′ ends within the 3′ UTR and identification of oligo(U) tails. The mapping experiment is the same as in Fig. 5. (A) Structure of the *GPEET* 3′ UTR [20]. Negative elements present in stem-loop LII are indicated: GRE (empty circles) and 26mer (filled circles). Location of 3′ ends (empty arrowheads, sites 1–9) and sites of oligo(U) tail addition (filled arrowheads, sites A–C) are shown. (B) Identification of 3′ ends in individual samples. (C) Identification of oligo(U) tails in individual samples. Circles depict numbers of clones obtained: 1 clone (empty circle), 2–6 clones (filled circle) and >12 clones (2 filled circles).

and that this might have resulted in false priming at uridine stretches. It was further proposed that this might be the origin of non-templated oligo(U) tails. Oligo-uridylated transcripts were also identified when a truncated primer was used, however, or a different linker and reverse primer (S.K., unpublished data), arguing against the oligo(U) tails being artifacts. Although we cannot completely rule out alternative explanations for our findings, it is worth mentioning that linker ligation/RT-PCR is the established methodology for detecting non-templated oligo(U) stretches in yeast, Arabidopsis and mammalian cells (for example, [44]).

4. Discussion

This study delivers insights into the sequence of events that occurs when early PF differentiate to late PF. The simultaneous analysis of EdU incorporation and GPEET expression demonstrated that, upon triggering differentiation, early PF first underwent growth arrest, then became GPEET-negative, and eventually resumed proliferation as late PF (Fig. 1C and D). Thus, the transition from early to late PF shares features with the differentiation of bloodstream forms to PF, which also follow a set sequence of events: proliferating long slender forms, which have a coat of VSG, first stop dividing, then exchange their surface coat from VSG to procyclins and, finally, resume proliferation [8,11,45].

An important aspect in the control of gene expression is the differential regulation of mRNA turnover between life-cycle stages. For the first time, we determined the abundance and stability of both *EP* and *GPEET* mRNA during differentiation from early to late PF (Figs. 2, 4, S1 and S2). Compared to early PF, *EP* mRNA abundance in late PF increased 2.4–2.8-fold, while a 25–50-fold reduction was observed for *GPEET*, as determined in different sets of experiments. In early PF, *GPEET* mRNA was extraordinarily stable ($t_{1/2}$ > 6 h), while *EP* had a $t_{1/2}$ of 2.31 h ± 0.11 (Fig. 2B). The opposite situation was observed in late PF: the $t_{1/2}$ of *GPEET* was markedly reduced ($t_{1/2}$ = 3.80 h ± 0.32) and *EP* was stabilised ($t_{1/2}$ > 6 h). The $t_{1/2}$ of procyclin mRNAs were thus longer than the $t_{1/2}$ of bulk procyclin mRNA previously determined in PF of the Lister 427 strain ($t_{1/2}$ ~ 60 min) [25]. This difference might be at least partly explained by the shorter generation time of Lister 427 compared to the AnTat1.1 strain (generation time of 9 h versus 17 h). Invariably, we found that *GPEET* mRNA in early PF was more stable than *EP* mRNA in both early and late PF.

Several studies revealed a biphasic decay pattern for *EP1* mRNA in bloodstream forms and identified the nucleases involved [27–29,46]. In one of our experiments, a decay pattern reminiscent of biphasic decay kinetics was found for *GPEET* mRNA in late PF (with only 0.4% GPEET-positive cells) (Fig. 4D). However, we observed some variability in mRNA turnover between different sets of experiments; for example, the experiments shown in Fig. 2B suggested a higher stability for *GPEET* in late PF (compare with Fig. 4D). These differences might be explained by the varying proportions of 'laggard' parasites that still expressed GPEET in late PF cultures: the more cells that are still GPEET-positive, the more highly stable *GPEET* mRNA would be present. The mRNA turnover observed in late PF cultures thus most likely represents an overlay of the $t_{1/2}$ of both GPEET-positive and -negative cells. Accordingly, the actual mRNA stability in GPEET-negative cells would be lower than determined in our study. Two sets of data argue against the *GPEET* mRNA detected in late PF cultures originating solely from the small fraction of 'laggard' GPEET-positive cells. First, the stability is markedly reduced in late PF compared to early PF. Second, mapping *GPEET* 3′ ends yielded an enrichment of alternatively processed transcripts in late PF.

It was proposed that both the 26mer, a negative element present in all procyclin 3′ UTRs [24,30], and the GRE, which is restricted to the *GPEET* 3′ UTR [20], might be targets for endonucleolytic cleavage or recruitment sites for distal cleavage by endonuclease(s) [23,25,47]. An identical mechanism was considered for the fast decay of *EP1* mRNA in bloodstream form *T. brucei* [26], but this was not confirmed by a subsequent study [28]. However, degradation of unstable *Leishmania* transcripts bearing a retroposon-derived instability motif in their 3′ UTR appears to be initiated by endonucleolytic cleavages at discrete sites [48]. We identified 9 different 3′ ends within the *GPEET* 3′ UTR (Fig. 6A and B). Among these, one site within the GRE was indeed enriched in samples from late PF cultures 6 h after addition of ActD. However, we cannot distinguish between (multiple) endonucleolytic cleavage(s) or 3′ to 5′ exonucleolytic degradation intermediates.

As expected from other systems/organisms, mapping *GPEET* mRNA 3′ ends revealed that poly(A) tails were shortened or completely removed after 6 h of transcription inhibition (Fig. 5A). While fewer adenylated sequences were obtained from late PF cultures, untailed 3′ UTRs that extended beyond the major polyadenylation site were only found in this life-cycle stage (Fig. 5B). A possible explanation might be that processing of *GPEET* transcripts is altered in late PF, thus preventing the generation of mature mRNA. Interestingly, the genomic organisation of *GPEET* and the adjacent *EP3* gene is unusual, as the intergenic region contains two distinct polypyrimidine stretches followed by a downstream AG dinucleotide, which both can function as polyadenylation/splice acceptor sites [41,49]. *Trans*-splicing of *EP3* mRNA can thus be uncoupled from 3′ end formation of the upstream *GPEET* mRNA, permitting

alternative processing of *GPEET* transcripts in late PF without interfering with *EP3* maturation.

Interestingly, our study identified the presence of non-templated oligo-uridylyl tails at three separate locations within the *GPEET* 3′ UTR (Fig. 6A and C), with a tail length of 8–13 Us. Furthermore, the most frequent oligo(U) tail was enriched in late PF cultures 6 h after addition of ActD. Why did transcriptome-wide analyses previously performed in *T. brucei* [42,43] not identify the uridylyl tails? One possibility is that the mapping algorithms employed resulted in annotation of the sequences as non-assignable reads and might have been ignored. In kinetoplastids, oligo(U) tails have been described for mitochondrial transcripts [50–53]. While uridylation of guide RNAs did not affect their stability, addition of up to 16 Us to the non-edited *ND1* mRNA by TbRET1 appeared to have a destabilising effect [53]; the function of oligo(U) tails in stability of mitochondrial mRNAs was shown to be transcript-specific, however [54]. Uridylation of both mRNAs and non-coding RNA species like U6 small nucleolar RNA, microRNAs and short interfering RNAs has been reported in various eukaryotes and was mainly implicated in controlling the stability and/or processing of these RNAs [55–58]. Moreover, it was proposed that cytoplasmic addition of U-tails to mRNAs might protect the 3′ end from degradation, and thus participates in establishing a 5′ to 3′ polarity of mRNA decay [44,58]. It is tempting to speculate that oligo(U) tails of *GPEET* mRNA elicit a similar degradation mechanism in late procyclic forms. To the best of our knowledge, this is the first study reporting a U-tailed, nuclear-encoded mRNA species in trypanosomatids or any other protozoa. The protein(s) responsible for the generation of oligo(U) tails as well as their function and significance requires further investigation. It also raises the question whether uridylation might be a signal for a specific RNA turnover pathway and if so, to what extent this mechanism is conserved with respect to other eukaryotes. Furthermore, it will be interesting to elucidate whether mRNAs encoding other differentially regulated genes might be uridylated in trypanosomes and *Leishmania*.

Acknowledgments

All lab members are thanked for their unwavering support during the past year. Marina Cristodero and Gaby Schumann are thanked for constructive comments on the manuscript and Antonio Estévez for encouragement and stimulating discussions. This research was supported by grants from the Swiss National Science Foundation and Howard Hughes Medical Institute to I.R.

References

[1] Shapiro SZ, Naessens J, Liesegang B, Moloo SK, Magondu J. Analysis by flow cytometry of DNA synthesis during the life cycle of African trypanosomes. Acta Trop 1984;41:313–23.
[2] Vickerman K. Polymorphism and mitochondrial activity in sleeping sickness trypanosomes. Nature 1965;208:762–6.
[3] Kabani S, Fenn K, Ross A, Ivens A, Smith TK, Ghazal P, et al. Genome-wide expression profiling of in vivo-derived bloodstream parasite stages and dynamic analysis of mRNA alterations during synchronous differentiation in *Trypanosoma brucei*. BMC Genom 2009;10:427.
[4] Tyler KM, Matthews KR, Gull K. The bloodstream differentiation-division of *Trypanosoma brucei* studied using mitochondrial markers. Proc Biol Sci: R Soc 1997;264:1481–90.
[5] Brown RC, Evans DA, Vickerman K. Changes in oxidative metabolism and ultrastructure accompanying differentiation of the mitochondrion in *Trypanosoma brucei*. Int J Parasitol 1973;3:691–704.
[6] Gunasekera K, Wüthrich D, Braga-Lagache S, Heller M, Ochsenreiter T. Proteome remodelling during development from blood to insect-form *Trypanosoma brucei* quantified by SILAC and mass spectrometry. BMC Genom 2012;13:556.
[7] Turner CM, Barry JD, Vickerman K. Loss of variable antigen during transformation of *Trypanosoma brucei rhodesiense* from bloodstream to procyclic forms in the tsetse fly. Parasitol Res 1988;74:507–11.
[8] Ziegelbauer K, Quinten M, Schwarz H, Pearson TW, Overath P. Synchronous differentiation of *Trypanosoma brucei* from bloodstream to procyclic forms in vitro. Eur J Biochem/FEBS 1990;192:373–8.
[9] Overath P, Czichos J, Stock U, Nonnengaesser C. Repression of glycoprotein synthesis and release of surface coat during transformation of *Trypanosoma brucei*. EMBO J 1983;2:1721–8.
[10] Bülow R, Nonnengässer C, Overath P. Release of the variant surface glycoprotein during differentiation of bloodstream to procyclic forms of *Trypanosoma brucei*. Mol Biochem Parasitol 1989;32:85–92.
[11] Roditi I, Schwarz H, Pearson TW, Beecroft RP, Liu MK, Richardson JP, et al. Procyclin gene expression and loss of the variant surface glycoprotein during differentiation of *Trypanosoma brucei*. J Cell Biol 1989;108:737–46.
[12] Roditi I, Clayton C. An unambiguous nomenclature for the major surface glycoproteins of the procyclic form of *Trypanosoma brucei*. Mol Biochem Parasitol 1999;103:99–100.
[13] Mowatt MR, Clayton CE. Developmental regulation of a novel repetitive protein of *Trypanosoma brucei*. Mol Cell Biol 1987;7:2838–44.
[14] Roditi I, Carrington M, Turner M. Expression of a polypeptide containing a dipeptide repeat is confined to the insect stage of *Trypanosoma brucei*. Nature 1987;325:272–4.
[15] Roditi I, Lehane MJ. Interactions between trypanosomes and tsetse flies. Curr Opin Microbiol 2008;11:345–51.
[16] Vassella E, Den Abbeele JV, Bütikofer P, Kunz Renggli C, Furger A, Brun R, et al. A major surface glycoprotein of *Trypanosoma brucei* is expressed transiently during development and can be regulated post-transcriptionally by glycerol or hypoxia. Genes Dev 2000;14:615–26.
[17] Bütikofer P, Vassella E, Ruepp S, Boschung M, Civenni G, Seebeck T, et al. Phosphorylation of a major GPI-anchored surface protein of *Trypanosoma brucei* during transport to the plasma membrane. J Cell Sci 1999;112(Pt 11):1785–95.
[18] Vassella E, Acosta-Serrano A, Studer E, Lee SH, Englund PT, Roditi I. Multiple procyclin isoforms are expressed differentially during the development of insect forms of *Trypanosoma brucei*. J Mol Biol 2001;312:597–607.
[19] Morris JC, Wang Z, Drew ME, Englund PT. Glycolysis modulates trypanosome glycoprotein expression as revealed by an RNAi library. EMBO J 2002;21:4429–38.
[20] Vassella E, Probst M, Schneider A, Studer E, Kunz Renggli C, Roditi I. Expression of a major surface protein of *Trypanosoma brucei* insect forms is controlled by the activity of mitochondrial enzymes. Mol Biol Cell 2004;15:3986–93.
[21] Urwyler S, Vassella E, Van Den Abbeele J, Kunz Renggli C, Blundell P, Barry JD, et al. Expression of procyclin mRNAs during cyclical transmission of *Trypanosoma brucei*. PLoS Pathogen 2005;1:e22.
[22] Bütikofer P, Ruepp S, Boschung M, Roditi I. 'GPEET' procyclin is the major surface protein of procyclic culture forms of *Trypanosoma brucei brucei* strain 427. Biochem J 1997;326:415–23.
[23] Schumann Burkard G, Käser S, de Araujo PR, Schimanski B, Naguleswaran A, Knüsel S, et al. Nucleolar proteins regulate stage-specific gene expression and ribosomal RNA maturation in *Trypanosoma brucei*. Mol Microbiol 2013;88:827–40.
[24] Hotz HR, Hartmann C, Huober K, Hug M, Clayton C. Mechanisms of developmental regulation in *Trypanosoma brucei*: a polypyrimidine tract in the 3′-untranslated region of a surface protein mRNA affects RNA abundance and translation. Nucleic Acids Res 1997;25:3017–26.
[25] Furger A, Schürch N, Kurath U, Roditi I. Elements in the 3′ untranslated region of procyclin mRNA regulate expression in insect forms of *Trypanosoma brucei* by modulating RNA stability and translation. Mol Cell Biol 1997;17:4372–80.
[26] Irmer H, Clayton C. Degradation of the unstable EP1 mRNA in *Trypanosoma brucei* involves initial destruction of the 3′-untranslated region. Nucleic Acids Res 2001;29:4707–15.
[27] Li CH, Irmer H, Gudjonsdottir-Planck D, Freese S, Salm H, Haile S, et al. Roles of a *Trypanosoma brucei* 5′ → 3′ exoribonuclease homolog in mRNA degradation. RNA 2006;12:2171–86.
[28] Schwede A, Manful T, Jha BA, Helbig C, Bercovich N, Stewart M, et al. The role of deadenylation in the degradation of unstable mRNAs in trypanosomes. Nucleic Acids Res 2009;37:5511–28.
[29] Haile S, Estevez AM, Clayton C. A role for the exosome in the *in vivo* degradation of unstable mRNAs. RNA 2003;9:1491–501.
[30] Schürch N, Furger A, Kurath U, Roditi I. Contributions of the procyclin 3′ untranslated region and coding region to the regulation of expression in bloodstream forms of *Trypanosoma brucei*. Mol Biochem Parasitol 1997;89:109–21.
[31] Le Ray D, Barry JD, Easton C, Vickerman K. First tsetse fly transmission of the AnTat serodeme of *Trypanosoma brucei*. Annales de la Societe belge de medecine tropicale 1977;57:369–81.
[32] Vassella E, Oberle M, Urwyler S, Kunz Renggli C, Studer E, Hemphill A, et al. Major surface glycoproteins of insect forms of *Trypanosoma brucei* are not essential for cyclical transmission by tsetse. PLoS One 2009;4:e4493.
[33] Vassella E, Boshart M. High molecular mass agarose matrix supports growth of bloodstream forms of pleomorphic *Trypanosoma brucei* strains in axenic culture. Mol Biochem Parasitol 1996;82:91–105.
[34] Brun R, Schönenberger M. Stimulating effect of citrate and *cis*-Aconitate on the transformation of *Trypanosoma brucei* bloodstream forms to procyclic forms *in vitro*. Zeitschrift fur Parasitenkunde (Berlin, Germany) 1981;66:17–24.
[35] Brun R, Schönenberger. Cultivation and in vitro cloning or procyclic culture forms of *Trypanosoma brucei* in a semi-defined medium. Short communication. Acta Trop 1979;36:289–92.

[36] Chomczynski P, Sacchi N. Single-step method of RNA isolation by acid guanidinium thiocyanate-phenol-chloroform extraction. Anal Biochem 1987;162:156–9.
[37] Flück C, Salomone JY, Kurath U, Roditi I. Cycloheximide-mediated accumulation of transcripts from a procyclin expression site depends on the intergenic region. Mol Biochem Parasitol 2003;127:93–7.
[38] Ruepp S, Furger A, Kurath U, Kunz Renggli C, Hemphill A, Brun R, et al. Survival of *Trypanosoma brucei* in the tsetse fly is enhanced by the expression of specific forms of procyclin. J Cell Biol 1997;137:1369–79.
[39] Hehl A, Vassella E, Braun R, Roditi I. A conserved stem-loop structure in the 3′ untranslated region of procyclin mRNAs regulates expression in *Trypanosoma brucei*. Proc Natl Acad Sci USA 1994;91:370–4.
[40] Burchmore RJ, Landfear SM. Differential regulation of multiple glucose transporter genes in *Leishmania mexicana*. J Biol Chem 1998;273:29118–26.
[41] Schürch N, Hehl A, Vassella E, Braun R, Roditi I. Accurate polyadenylation of procyclin mRNAs in *Trypanosoma brucei* is determined by pyrimidine-rich elements in the intergenic regions. Mol Cell Biol 1994;14:3668–75.
[42] Siegel TN, Hekstra DR, Wang X, Dewell S, Cross GA. Genome-wide analysis of mRNA abundance in two life-cycle stages of *Trypanosoma brucei* and identification of splicing and polyadenylation sites. Nucleic Acids Res 2010;38:4946–57.
[43] Kolev NG, Franklin JB, Carmi S, Shi H, Michaeli S, Tschudi C. The transcriptome of the human pathogen *Trypanosoma brucei* at single-nucleotide resolution. PLoS Pathogen 2010;6:e1001090.
[44] Sement FM, Ferrier E, Zuber H, Merret R, Alioua M, Deragon JM, et al. Uridylation prevents 3′ trimming of oligoadenylated mRNAs. Nucleic Acids Res 2013;41:7115–27.
[45] Matthews KR, Gull K. Evidence for an interplay between cell cycle progression and the initiation of differentiation between life cycle forms of African trypanosomes. J Cell Biol 1994;125:1147–56.
[46] Schwede A, Ellis L, Luther J, Carrington M, Stoecklin G, Clayton C. A role for Caf1 in mRNA deadenylation and decay in trypanosomes and human cells. Nucleic Acids Res 2008;36:3374–88.
[47] Roditi I, Furger A, Ruepp S, Schürch N, Bütikofer P. Unravelling the procyclin coat of *Trypanosoma brucei*. Mol Biochem Parasitol 1998;91:117–30.
[48] Müller M, Padmanabhan PK, Rochette A, Mukherjee D, Smith M, Dumas C, et al. Rapid decay of unstable Leishmania mRNAs bearing a conserved retroposon signature 3′-UTR motif is initiated by a site-specific endonucleolytic cleavage without prior deadenylation. Nucleic Acids Res 2010;38:5867–83.
[49] Vassella E, Braun R, Roditi I. Control of polyadenylation and alternative splicing of transcripts from adjacent genes in a procyclin expression site: a dual role for polypyrimidine tracts in trypanosomes. Nucleic Acids Res 1994;22:1359–64.
[50] Blum B, Simpson L. Guide RNAs in kinetoplastid mitochondria have a nonencoded 3′ oligo(U) tail involved in recognition of the preedited region. Cell 1990;62:391–7.
[51] Adler BK, Harris ME, Bertrand KI, Hajduk SL. Modification of *Trypanosoma brucei* mitochondrial rRNA by posttranscriptional 3′ polyuridine tail formation. Mol Cell Biol 1991;11:5878–84.
[52] Madej MJ, Alfonzo JD, Huttenhofer A. Small ncRNA transcriptome analysis from kinetoplast mitochondria of *Leishmania tarentolae*. Nucleic Acids Res 2007;35:1544–54.
[53] Aphasizheva I, Aphasizhev R. RET1-catalyzed uridylylation shapes the mitochondrial transcriptome in *Trypanosoma brucei*. Mol Cell Biol 2010;30:1555–67.
[54] Zimmer SL, McEvoy SM, Menon S, Read LK. Additive and transcript-specific effects of KPAP1 and TbRND activities on 3′ non-encoded tail characteristics and mRNA stability in *Trypanosoma brucei*. PLoS One 2012;7:e37639.
[55] Marzluff W. A new way to initiate mRNA degradation. Nat Struct Mol Biol 2009;16:613–4.
[56] Wilusz CJ, Wilusz J. New ways to meet your (3′) end: oligouridylation as a step on the path to destruction. Genes Dev 2008;22:1–7.
[57] Morozov IY, Caddick MX. Cytoplasmic mRNA 3′ tagging in eukaryotes: does it spell the end. Biochem Soc Trans 2012;40:810–4.
[58] Norbury CJ. 3′ uridylation and the regulation of RNA function in the cytoplasm. Biochem Soc Trans 2010;38:1150–3.